Learning Fair Invariant Representations under Covariate and Correlation Shifts Simultaneously

Dong Li
Tianjin University
Tianjin, China
li13255486422@gmail.com

Chen Zhao
Baylor University
Waco, Texas, USA
chen_zhao@baylor.edu

Minglai Shao*
Tianjin University
Tianjin, China
shaoml@tju.edu.cn

Wenjun Wang*
Tianjin University
Tianjin, China
13255486722@163.com

Abstract

Achieving the generalization of an invariant classifier from training domains to shifted test domains while simultaneously considering model fairness is a substantial and complex challenge in machine learning. Existing methods address the problem of fairness-aware domain generalization, focusing on either covariate shift or correlation shift, but rarely consider both at the same time. In this paper, we introduce a novel approach that focuses on learning a fairness-aware domain-invariant predictor within a framework addressing both covariate and correlation shifts simultaneously, ensuring its generalization to unknown test domains inaccessible during training. In our approach, data are first disentangled into content and style factors in latent spaces. Furthermore, fairness-aware domain-invariant content representations can be learned by mitigating sensitive information and retaining as much other information as possible. Extensive empirical studies on benchmark datasets demonstrate that our approach surpasses state-of-the-art methods with respect to model accuracy as well as both group and individual fairness.

CCS Concepts

• **Computing methodologies** → *Learning under covariate shift*; *Learning latent representations.*

Keywords

Algorithmic Learning, Domain Generalization, Invariance, Covariate Shift, Correlation Shift

ACM Reference Format:
Dong Li, Chen Zhao, Minglai Shao, and Wenjun Wang. 2024. Learning Fair Invariant Representations under Covariate and Correlation Shifts Simultaneously. In *Proceedings of the 33rd ACM International Conference on Information and Knowledge Management (CIKM '24), October 21–25, 2024, Boise, ID, USA.* ACM, New York, NY, USA, 10 pages. https://doi.org/10.1145/3627673.3679727

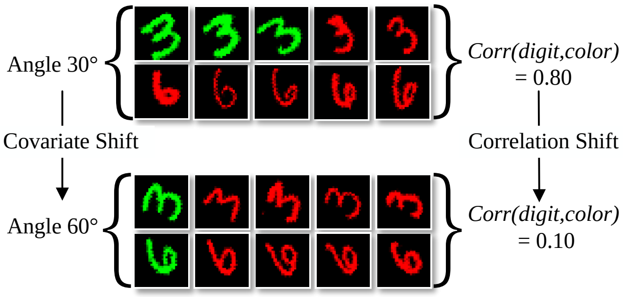

Figure 1: Taking a digit dataset (*e.g.* RCMNIST) as an example to illustrate covariate shift and correlation shift across domains. Here, domain is uniquely determined by the rotation angle and $Corr(digit, color)$, the color serves as the sensitive attribute. $Corr(digit, color)$ represents the correlation between the digit (3 and 6) and color (red and green).

1 Introduction

While machine learning has achieved remarkable success in various areas, including computer vision [14], natural language processing [5], and many others [10, 11, 35], these accomplishments are often built upon the assumption that training and test data are independently and identically distributed (*i.i.d.*) within their respective domains [33].

However, models under this assumption tend to perform poorly when there is a distribution shift between the training and test domains. Addressing distribution shifts across domains and generalizing from finite training domains to unseen but related test domains is the primary goal of domain generalization (DG) [1].

Many types of distribution shift are introduced in [20], such as label shift [34], concept shift [36], covariate shift [30], and correlation shift [28]. The covariate shift is defined as the differences in the marginal distributions over instances across different domains [30]. As shown in Figure 1, the two domains exhibit variations resulting from different image styles, represented by varying rotation angles. Correlation shift is defined as the variation in the dependency between the sensitive attribute and label across domains. For example, in Figure 1, it is evident that there is a strong correlation between the digit (3,6) and digit colors (green, red) when rotated at 30°, whereas this correlation becomes less pronounced at 60°.

Since the correlation involves sensitive attributes, correlation shift is highly related to fairness. In the context of algorithmic decision-making, fairness means the absence of any bias or favoritism towards an individual or group based on their inherent or acquired characteristics [23]. Many methods have been proposed to address the domain generalization (DG) problem [1, 17, 18, 31, 39],

[*] Corresponding authors

CIKM '24, October 21–25, 2024, Boise, ID, USA

ACM ISBN 979-8-4007-0436-9/24/10
https://doi.org/10.1145/3627673.3679727

but most of them lack fairness considerations. Therefore, when these algorithms are applied in human-centered real-world settings, they may exhibit bias against populations [12] characterized by sensitive features, such as gender and race.

While existing efforts have addressed the challenge of fairness-aware domain generalization due to shifted domains, they either overlook the variation in data across domains in the marginal distribution of data features [4, 25] or specifically address the spurious correlation between sensitive attributes and predicted outcomes in terms of unchanged group fairness [26] across domains. Therefore, research is needed to explore fairness-aware domain generalization considering both covariate and correlation shifts simultaneously across training and test domains.

In this paper, we propose a novel framework, namely Fairness-aware LeArning Invariant Representations (FLAIR). It focuses on the problem arising from both covariate shift and correlation shift while considering fairness. The overall framework is shown in Figure 2. In the presence of multiple training domains, our objective is to acquire a predictor that is both domain-invariant and fairness-aware. This enables effective generalization in unseen test domains while preserving both accuracy and fairness. We assume there exists an underlying transformation model that can transform instances sampled from one domain to another while keeping the class labels unchanged. Under this assumption, the predictor consists of three components: a content featurizer, a fair representation learner, and an invariant classifier. To achieve fairness, data are divided into different sensitive subgroups. Within each subgroup, content factors encoded from the content featurizer are reconstructed using K latent prototypes. These reconstructed content representations over various sensitive subgroups are crafted with dual objectives: (1) minimizing the inclusion of sensitive information and (2) maximizing the preservation of non-sensitive information. Utilizing these representations as inputs, we train a fairness-aware domain-invariant classifier for making model predictions. Exhausted experiments showcase that FLAIR demonstrates robustness in the face of covariate shift, even when facing alterations in unfairness and correlation shift across domains. The main contributions are summarized:

- We introduce a fairness-aware domain generalization problem within a framework that addresses both covariate and correlation shifts simultaneously, which has practical significance.
- We introduce an end-to-end training approach aimed at learning a fairness-aware domain invariant predictor. We claim that the trained predictor can generalize effectively to unseen test domains that are unknown and inaccessible during training.
- Comprehensive experiments on three benchmark datasets show that our proposed algorithm FLAIR significantly outperforms state-of-the-art baselines with respect to model accuracy as well as both group and individual fairness.

2 Related Work

Algorithmic Fairness in Machine Learning. In recent years, fairness in machine learning has gained widespread attention. In this field, there is a widely recognized trade-off: enhancing fairness may come at the cost of accuracy to some extent [3, 24]. How to handle such a trade-off, especially in real-world datasets, has been a widely researched issue in the field of algorithmic fairness.

From a statistical perspective, algorithmic fairness metrics are typically divided into group fairness and individual fairness. The conflict between them is a common challenge, as algorithms that achieve group fairness may not be able to handle individual fairness [15]. LFR [38] is the first method to achieve both group fairness and individual fairness simultaneously. It encodes tabular data, aiming to preserve the original data as much as possible while ignoring information related to sensitive attributes.

Fairness-Aware Domain Generalization. Some efforts [40–44] have already been attempted to address the fairness-aware domain generalization problem. EIIL [4] takes correlation shift into consideration when addressing the DG problem, thus ensuring fairness to some extent. FVAE [25] learns fair representation through contrastive learning and both improve out-of-distribution generalization and fairness. But both of them only take correlation shift into account while assuming that covariate shift remains invariant. The latest work FATDM [26] attempts to simultaneously enhance the model's accuracy and fairness, considering the DG problem associated with covariate shift. However, it does not consider correlation shift and solely focuses on group fairness, without addressing individual fairness.

3 Preliminaries

Notations. Let $\mathcal{X} \subseteq \mathbb{R}^d$ denote a feature space, $\mathcal{A} = \{-1, 1\}$ is a sensitive space, and $\mathcal{Y} = \{0, 1\}$ is a label space for classification. Let $\mathcal{C} \subseteq \mathbb{R}^c$ and $\mathcal{S} \subseteq \mathbb{R}^s$ be the latent content and style spaces, respectively, induced from $\mathcal{X}$ by an underlying transformation model $T : \mathcal{X} \times \mathcal{X} \to \mathcal{X}$. We use X, A, Y, C, S to denote random variables that take values in $\mathcal{X}, \mathcal{A}, \mathcal{Y}, \mathcal{C}, \mathcal{S}$ and $\mathbf{x}, a, y, \mathbf{c}, \mathbf{s}$ be the realizations. A domain $e \in \mathcal{E}$ is specified by distribution $\mathbb{P}(X^e, A^e, Y^e) : \mathcal{X} \times \mathcal{A} \times \mathcal{Y} \to [0, 1]$. A predictor f parameterized by $\boldsymbol{\theta}_{cls}$ denotes $f : \mathcal{X} \times \mathcal{A} \times \Theta \to \mathcal{Y}$.

Problem Formulation. We consider a set of data domains $\mathcal{E}$, where each domain $e \in \mathcal{E}$ corresponds to a distinct data $\mathcal{D}^e = \{(\mathbf{x}_i^e, a_i^e, y_i^e)\}_{i=1}^{|\mathcal{D}^e|}$ sampled *i.i.d.* from $\mathbb{P}(X^e, A^e, Y^e)$. Given a dataset $\mathcal{D} = \{\mathcal{D}^e\}_{e \in \mathcal{E}}$, it is partitioned into a training dataset $\mathcal{D}_{tr} \subset \mathcal{D}$ with multiple training domains $\mathcal{E}_{tr} \subset \mathcal{E}$ and a test dataset $\mathcal{D}_{te} = \mathcal{D} \backslash \mathcal{D}_{tr}$ with unknown test domains which are inaccessible during training. Therefore, given samples from finite training domains, we aim to learn a fairness-aware predictor f at training that is generalizable on unseen test domains.

Problem 1 (Domain generalization concerning fairness). *Let $\mathcal{E}_{tr} \subset \mathcal{E}$ be a finite subset of training domains and assume that for each $e \in \mathcal{E}_{tr}$, we have access to its corresponding data $\mathcal{D}^e = \{(\mathbf{x}_i^e, a_i^e, y_i^e)\}_{i=1}^{|\mathcal{D}^e|}$ sampled i.i.d. from $\mathbb{P}(X^e, A^e, Y^e)$. Given a loss function $\ell_{CE} : \mathcal{Y} \times \mathcal{Y} \to \mathbb{R}$, the goal is to learn a fair predictor f parameterized by $\boldsymbol{\theta}_{cls} \in \Theta_{fair} \subset \Theta$ for any $\mathcal{D}^e \in \mathcal{D}_{tr}$ that minimizes the worst-case risk over training domains $\mathcal{E}_{tr}$ that*

$$\min_{\boldsymbol{\theta}_{cls} \in \Theta_{fair}} \max_{e \in \mathcal{E}_{tr}} \mathbb{E}_{\mathbb{P}(X^e, A^e, Y^e)} \ell_{CE}(f(X^e, A^e, \boldsymbol{\theta}_{cls}), Y^e)$$

However, addressing Problem 1 by training such a predictor f is challenging because (1) f is required to remain invariant across domains in terms of model accuracy, and model outcomes are fair with respect to sensitive subgroups defined by A; and (2) we do not assume data from $\mathcal{E} \backslash \mathcal{E}_{tr}$ is accessible during training.

To tackle such challenges, we divide the fairness-aware domain invariant predictor f into three components: a domain-invariant featurizer $h_c : \mathcal{X} \times \Theta_{fair} \to \mathcal{C}$ parameterized by $\boldsymbol{\theta}_c$, a fair representation learner $g : \mathcal{C} \times \mathcal{A} \times \Theta_{fair} \to \mathcal{C}$ parameterized by $\boldsymbol{\theta}_g$, and a classifier $\omega : \mathcal{C} \times \Theta_{fair} \to \mathbb{R}$ parameterized by $\boldsymbol{\theta}_w$, denoted $f = h_c \circ g \circ \omega$ and $\boldsymbol{\theta}_{cls} = \{\boldsymbol{\theta}_c, \boldsymbol{\theta}_g, \boldsymbol{\theta}_w\}$.

4 Fairness-aware Learning Invariant Representations (FLAIR)

In this paper, we narrow the scope of various distribution shifts and focus on a hybrid shift where covariate and correlation shifts are present simultaneously.

Definition 1 (Covariate shift and correlation shift). *Given $\forall e_1, e_2 \in \mathcal{E}$ and $e_1 \neq e_2$, a covariate shift occurs in Problem 1 when domain variation is due to differences in the marginal distributions over input features $\mathbb{P}(X^{e_1}) \neq \mathbb{P}(X^{e_2})$. Meanwhile, a correlation shift arises in Problem 1 when domain variation results from changes in the joint distribution between Y and Z, denoted as $\mathbb{P}(A^{e_1}, Y^{e_1}) \neq \mathbb{P}(A^{e_2}, Y^{e_2})$. More specifically, $\mathbb{P}(Y^{e_1}|A^{e_1}) \neq \mathbb{P}(Y^{e_2}|A^{e_2})$ and $\mathbb{P}(A^{e_1}) = \mathbb{P}(A^{e_2})$; or $\mathbb{P}(A^{e_1}|Y^{e_1}) \neq \mathbb{P}(A^{e_2}|Y^{e_2})$ and $\mathbb{P}(Y^{e_1}) = \mathbb{P}(Y^{e_2})$.*

In Section 4.1, we handle covariate shift by enforcing invariance on instances based on disentanglement, while in Section 4.2, we address correlation shift by learning fair content representation.

4.1 Disentanglement of Domain Variation

In [27], distribution shifts are attributed into two forms: concept shift, where the distribution of instance classes varies across different domains, and covariate shift, where the marginal distributions over instance $\mathbb{P}(X^e)$ are various. In this paper, we restrict the scope of our framework to focus on Problem 1 in which inter-domain variation is solely due to covariate shift.

Building upon the insights from existing domain generalization literature [27, 39, 44], data variations across domains are disentangled into multiple factors in latent spaces.

Assumption 1 (Latent Factors). *Given $\mathcal{D}^e = \{(\mathbf{x}_i^e, a_i^e, y_i^e)\}_{i=1}^{|\mathcal{D}^e|}$ sampled i.i.d. from $\mathbb{P}(X^e, A^e, Y^e)$ in domain $e \in \mathcal{E}$, we assume that each instance $(\mathbf{x}_i^e, a_i^e, y_i^e)$ is generated from*

- *a latent content factor $\mathbf{c} = h_c(\mathbf{x}_i^e, \boldsymbol{\theta}_c) \in \mathcal{C}$, where $\mathcal{C} = \{\mathbf{c}_{y=0}, \mathbf{c}_{y=1}\}$ refers to a content space, and h_c is a content encoder;*
- *a latent style factor $\mathbf{s}^e = h_s(\mathbf{x}_i^e, \boldsymbol{\theta}_s) \in \mathcal{S}$, where $\mathbf{s}^e$ is specific to the individual domain e, and $h_s : \mathcal{X} \times \Theta \to \mathcal{S}$ is a style encoder.*

We assume that the content factors in $\mathcal{C}$ do not change across domains. Each domain e over $\mathbb{P}(X^e, A^e, Y^e)$ is represented by a unique $\mathbf{s}^e$ and $Corr(Y^e, A^e)$, where $Corr(Y^e, A^e)$ is the correlation betweem Y^e and A^e.

Under Assumption 1, we further assume that, for any two domains $e_i, e_j \in \mathcal{E}$, inter-domain variations between them due to covariate shift are managed via an underlying transformation model T. Through this model, instances sampled from such two domains can be transformed interchangeably.

Assumption 2 (Transformation Model). *We assume, $\forall e, e' \in \mathcal{E}, e \neq e'$, there exists a function $T : \mathcal{X} \times \mathcal{X} \to \mathcal{X}$ that transforms instances from domain e to e', denoted as $X^{e'} = T(X^e, X^{e'})$. The transformation model T is defined as*

$$T(X^e, X^{e'}) = D(h_c(X^e, \boldsymbol{\theta}_c), h_s(X^{e'}, \boldsymbol{\theta}_s), \boldsymbol{\theta}_d)$$

where h_c and h_s are content and style encoders defined in Assumption 1, and $D : \mathcal{C} \times \mathcal{S} \times \Theta \to \mathcal{X}$ denotes a decoder.

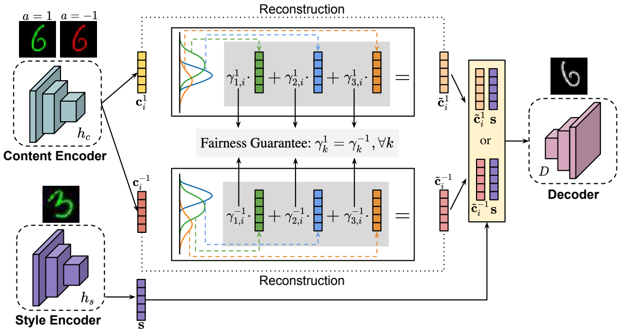
$a = 1$
$a = -1$
Reconstruction
$\mathbf{c}_i^1$
$\gamma_{1,i}^1 \cdot$ $+ \gamma_{2,i}^1 \cdot$ $+ \gamma_{3,i}^1 \cdot$ $=$
$\tilde{\mathbf{c}}_i^1$
h_c
Content Encoder
Fairness Guarantee: $\gamma_k^1 = \gamma_k^{-1}, \forall k$
$\mathbf{c}_i^{-1}$
$\gamma_{1,i}^{-1} \cdot$ $+ \gamma_{2,i}^{-1} \cdot$ $+ \gamma_{3,i}^{-1} \cdot$ $=$
$\tilde{\mathbf{c}}_i^{-1}$
$\tilde{\mathbf{c}}_i^1$ s
or
$\tilde{\mathbf{c}}_i^{-1}$ s
D
Decoder
h_s
Style Encoder
Reconstruction
s

Figure 2: Illustrating the pipeline of FLAIR using `RCMNIST` dataset as an example. The content encoder h_c first maps instances to the latent content space to obtain latent content factors. Subsequently, these content factors are grouped based on the sensitive attributes (color) into $\mathbf{c}_i^1$ and $\mathbf{c}_i^{-1}$. Consequently, the fair content representations $\tilde{\mathbf{c}}_i^1$ and $\tilde{\mathbf{c}}_i^{-1}$ are reconstructed using weighted prototypes. Each prototype represents a statistical mean estimated from its corresponding cluster, which is fitted by the content factors of the respective subgroups, while ensuring fairness through Eq.(4). Further, instances are transformed into different domains using the style factor s extracted by the style encoder h_s.

With the transformation model T that transforms instances from domain e to e', $\forall e, e' \in \mathcal{E}$, under Assumption 2, we introduce a new definition of invariance with respect to the variation captured by T in Definition 2.

Definition 2 (T-invariance). *Under Assumptions 1 and 2, given a transformation model T as well as two instance $(\mathbf{x}_i^e, a_i^e, y_i^e)$ and $(\mathbf{x}_j^{e'}, a_j^{e'}, y_j^{e'})$, a content encoder h_c is domain invariant if it holds*

$$\begin{aligned} \mathbf{x}_j^{e'} &= T(\mathbf{x}_i^e, \mathbf{x}_j^{e'}), \quad \text{when} \quad e \neq e', y^e = y^{e'}, \quad \text{or} \\ \mathbf{x}_i^{e} &= T(\mathbf{x}_i^e, \mathbf{x}_j^{e'}), \quad \text{when} \quad e = e', y^e \neq y^{e'} \end{aligned} \tag{1}$$

almost surely $\forall e, e' \in \mathcal{E}$.

Definition 2 is crafted to enforce invariance on instances based on disentanglement via T. The output of h_c is further utilized to acquire a fairness-aware representation, considering different sensitive subgroups, through the learner g within the content latent space.

4.2 Learning Fair Content Representations

Dwork et al., [6] defines fairness that *similar individuals are treated similarly.* As stated in Section 4.1, the featurizer h_c maps instances to the latent content space. Therefore, for each instance $(\mathbf{x}_i^e, a_i^e, y_i^e)$ sampled *i.i.d.* from $\mathbb{P}(X^e, A^e, Y^e)$ where $e \in \mathcal{E}_{tr}$, the goal of the learner g is to reconstruct a fair content representation $\tilde{\mathbf{c}}_i = g(\mathbf{c}_i, \boldsymbol{\theta}_g)$ from $\mathbf{c}_i = h_c(\mathbf{x}_i^e, \boldsymbol{\theta}_c)$, wherein $\tilde{\mathbf{c}}_i$ is generated to meet two objectives

(1) minimizing the information disclosure related to a specific sensitive subgroup $\mathcal{D}_{tr}^{a=-1}$ or $\mathcal{D}_{tr}^{a=1}$, and (2) maximizing the preservation of significant information within non-sensitive representations. Under Assumption 1, since the content space is invariant across domains, we omit the superscript of domain labels for content factors.

To achieve these objectives effectively through g and drawing inspiration from [15, 38], we group the content factors along with the sensitive attributes, denoted $\{\mathbf{c}_i^a\}_{i=1}^{N^a} = \{(\mathbf{c}_i, a_i)\}_{i=1}^{N^a}$, of instances $\{(\mathbf{x}_i^e, a_i^e, y_i^e)\}_{i=1}^{N^a}$ within each sensitive subgroup $\mathcal{D}_{tr}^a, \forall a \in \{-1, 1\}$, which are encoded from h_c, into K clusters based on their similarity. Consequently, their fair content representations $\{\tilde{\mathbf{c}}_i^a\}_{i=1}^{N^a}$, with the sensitive attributes $\{a_i\}_{i=1}^{N^a}$ unchanged, are reconstructed using weighted prototypes, with each prototype $\boldsymbol{\mu}_k^a$ representing a statistical mean estimated from each cluster.

Specifically, for content factors $\{\mathbf{c}_i^a\}_{i=1}^{N^a}$ in a sensitive subgroup a where $a \in \{-1, 1\}$, let Z be a latent variable, where its realization $\mathbf{z}^a \in \{0, 1\}^K$ is a K-dimensional vector, satisfying a particular entry z_k^a is equal to 1, while all other entries are set to 0s, and $\sum_k z_k^a = 1$. We denote π_k^a as the mixing coefficients representing the prior probability of $z_k^a = 1$ that $\mathbf{c}_i^a$ belongs to the k-th prototype.

$$\mathbb{P}(z_k^a = 1) = \pi_k^a, \quad 0 \leq \pi_k^a \leq 1, \quad \sum_{k=1}^{K} \pi_k^a = 1$$

In the context of Gaussian mixture models, we assume the conditional distribution $(C^a | Z^a = z_k^a) \sim \mathcal{N}(\boldsymbol{\mu}_k^a, \Sigma_k^a)$. To estimate the parameters $\boldsymbol{\theta}_g^a = \{\boldsymbol{\mu}_k^a, \Sigma_k^a, \pi_k^a\}_{k=1}^K$ of the subgroup a, we take the loss

$$\mathcal{L}_{gmm}(\mathbf{x}_i^a, \boldsymbol{\theta}_c, \boldsymbol{\theta}_g^a) = -\sum_{i=1}^{N^a} \ln \left\{ \sum_{k=1}^{K} \pi_k^a \mathcal{N}(\mathbf{c}_i^a | \boldsymbol{\mu}_k^a, \Sigma_k^a) \right\} + \sum_{k=1}^{K} \pi_k^a \tag{2}$$

Intuitively, the latent variable Z is the key to finding the maximal log-likelihood. We attempt to compute the posterior distribution $\gamma_{k,i}^a$ of Z given the observations $\mathbf{c}_i^a$:

$$\gamma_{k,i}^a := \mathbb{P}(z_k^a = 1 | \mathbf{c}_i^a) = \frac{\pi_k^a \mathcal{N}(\mathbf{c}_i^a | \boldsymbol{\mu}_k^a, \Sigma_k^a)}{\sum_{j=1}^{K} \pi_j^a \mathcal{N}(\mathbf{c}_i^a | \boldsymbol{\mu}_j^a, \Sigma_j^a)} \tag{3}$$

To achieve fairness, the fundamental idea designing g is to make sure that the probability that a random content factor $\mathbf{c}_i^{a=-1}$ from the sensitive subgroup $a = -1$ mapping to the k-th particular prototype $\boldsymbol{\mu}_k^{a=-1}$ is equal to the probability of a random content factor $\mathbf{c}_i^{a=1}$ mapping to the prototype $\boldsymbol{\mu}_k^{a=1}$ from the other sensitive subgroup $a = 1$.

$$\gamma_k^{a=1} = \gamma_k^{a=-1}, \forall k \quad \text{where } \gamma_k^a = \mathbb{E}_{(\mathbf{x}_i, a, y_i) \sim \mathbb{P}(X, A=a, Y)} \gamma_{k,i}^a \tag{4}$$

We hence formulate the loss regarding fairness that

$$\mathcal{L}_{fair}(\mathcal{D}_{tr}, \boldsymbol{\theta}_c, \boldsymbol{\theta}_g) = \sum_{k=1}^{K} \left| \gamma_k^{a=1} - \gamma_k^{a=-1} \right| \tag{5}$$

where $\boldsymbol{\theta}_g = \{\boldsymbol{\theta}_g^{a=-1}, \boldsymbol{\theta}_g^{a=1}\}$. Eq.(5) draws inspiration from the group fairness metric, known as the Difference of Demographic Parity (DDP) [21], which enforces the statistical parity between two sensitive subgroups.

To maximize the non-sensitive information in the reconstructed content representations, the reconstruction loss is defined

$$\begin{aligned} \mathcal{L}_{rec}(\mathbf{x}_i^a, \boldsymbol{\theta}_c, \boldsymbol{\theta}_g^a) &= \sum_{i=1}^{|\mathcal{E}_{tr}|} dist[\mathbf{c}_i^a, \tilde{\mathbf{c}}_i^a], \quad \forall a \in \{-1, 1\} \\ \text{where} \quad \tilde{\mathbf{c}}_i^a &= g(\mathbf{c}_i^a, \boldsymbol{\theta}_g^a) = \sum_{k=1}^{K} \gamma_{k,i}^a \cdot \boldsymbol{\mu}_k^a \end{aligned} \tag{6}$$

where $|\mathcal{E}_{tr}| = N^{a=-1} + N^{a=1}$ and $dist[\cdot, \cdot] : C \times C \to \mathbb{R}$ is the Euclidean distance metric.

4.3 Learning the Predictor f

To tackle Problem 1, which aims to learn a fairness-aware domain invariant predictor f, a crucial element of f is the acquisition of content factors through h_c, while simultaneously reducing the sensitive information associated with them through g. In this subsection, we introduce a framework designed to train f with a focus on both domain invariance and model fairness.

Given training domains $\mathcal{E}_{tr}$, a data batch $Q = \{(\mathbf{r}_1, \mathbf{r}_2, \mathbf{r}_3, \mathbf{r}_4)_q\}_{q=1}^{Q}$ containing multiple quartet instance pairs are sampled from $\mathbb{P}(X^e, A^e, Y^e)$ and $\mathbb{P}(X^{e'}, A^{e'}, Y^{e'}), \forall e, e' \in \mathcal{E}_{tr}$, where Q denotes the number of quartet pairs in $|Q|$. Specifically,

$$\begin{aligned} \mathbf{r}_1 &= (\mathbf{x}_1^e, a = -1, y), && \text{with class } y \text{ and domain } e \\ \mathbf{r}_2 &= (\mathbf{x}_2^e, a = 1, y'), && \text{with class } y' \text{ and domain } e \\ \mathbf{r}_3 &= (\mathbf{x}_3^{e'}, a = -1, y), && \text{with class } y \text{ and domain } e' \\ \mathbf{r}_4 &= (\mathbf{x}_4^{e'}, a = 1, y'), && \text{with class } y' \text{ and domain } e' \end{aligned}$$

We set $\mathbf{r}_1$ and $\mathbf{r}_2$ (same to $\mathbf{r}_3$ and $\mathbf{r}_4$) share the same domain e but different class label y and y', while $\mathbf{r}_1$ and $\mathbf{r}_3$ (same to $\mathbf{r}_2$ and $\mathbf{r}_4$) share the same class label y but different domains e and e'. Therefore, $\mathbf{r}_1$ and $\mathbf{r}_2$ are alternative instances with respect to $\mathbf{r}_3$ and $\mathbf{r}_4$ in a different domain, respectively.

Therefore, under Definition 2 and Eq.(1), we have the invariance loss R_{inv} with respect to $\boldsymbol{\theta}_{inv} = \{\boldsymbol{\theta}_c, \boldsymbol{\theta}_s, \boldsymbol{\theta}_d\}$,

$$R_{inv}(\boldsymbol{\theta}_{inv}) = \mathbb{E}_{(R1,R2,R3,R4) \in Q} \Big(d[R_1, T(R_1, R_2)] + d[R_3, T(R_3, R_4)] \Big) \tag{7}$$

Note that in each distance metric $d[\cdot]$ of R_{inv}, it compares a pair of instances with the same domain but different classes.

Furthermore, given Eq.(2), Eq.(6) and under Definition 2, we have the invariant classification loss with respect to $\boldsymbol{\theta}_{cls} = \{\boldsymbol{\theta}_c, \boldsymbol{\theta}_g, \boldsymbol{\theta}_w\}$,

$$R_{cls}(\boldsymbol{\theta}_{cls}) = R_{cls}(\boldsymbol{\theta}_{cls}^{a=-1}) + R_{cls}(\boldsymbol{\theta}_{cls}^{a=1}) \tag{8}$$

with

$$\begin{aligned} R_{cls}(\boldsymbol{\theta}_{cls}^a) = \mathbb{E}_{(R_i, R_j) \in Q} \Big\{ & d[R_i, T(R_i, R_j)] + \mathcal{L}_{gmm}(R_i, \boldsymbol{\theta}_c, \boldsymbol{\theta}_g^a) \\ & + \mathcal{L}_{rec}(R_i, \boldsymbol{\theta}_c, \boldsymbol{\theta}_g^a) + \ell_{CE}\Big(\omega(g(h_c(R_i, \boldsymbol{\theta}_c), \boldsymbol{\theta}_g^a), \boldsymbol{\theta}_w), Y\Big) \Big\} \end{aligned}$$

where $d : \mathcal{X} \times \mathcal{X} \to \mathbb{R}$ indicates a distance metric, such as ℓ_1-norm. $R_{cls}(\boldsymbol{\theta}_{cls}^{a=-1})$ indicates the empirical risk of instance pairs with the sensitive attribute $a = -1$. Similarly, $R_{cls}(\boldsymbol{\theta}_{cls}^{a=1})$ is the empirical risk of instance pairs with the sensitive attribute $a = 1$. Notice that the instance pair (R_i, R_j) in R_{cls} sampled from Q have the same class label but different domains, such as $(\mathbf{r}_1, \mathbf{r}_3)$ and $(\mathbf{r}_2, \mathbf{r}_4)$.

Algorithm 1 Fairness-aware Learning Invariant Representations (FLAIR)

```
    Input: Training dataset $\mathcal{D}_{tr}$, stepsize $\eta_1, \eta_2, \eta_3$, margin $\epsilon_1, \epsilon_2$,
    number of prototypes $K$
    Initialize: primal variables $\boldsymbol{\theta} = \{\boldsymbol{\theta}_c, \boldsymbol{\theta}_s, \boldsymbol{\theta}_d, \boldsymbol{\theta}_g, \boldsymbol{\theta}_w\}$ and dual
    variables $\lambda_1, \lambda_2$
 1: repeat
 2:     Sample a batch $Q = \{(\mathbf{r}_1, \mathbf{r}_2, \mathbf{r}_3, \mathbf{r}_4)_q\}_{q=1}^{Q}$ in $\mathcal{D}_{tr}$.
 3:     Evaluate $R_{inv}(\boldsymbol{\theta}_c, \boldsymbol{\theta}_s, \boldsymbol{\theta}_d)$ using $Q$ and Eq.(7).
 4:     Estimate $\boldsymbol{\theta}_g = \text{FairGMMs}(Q, \boldsymbol{\theta}_c)$
 5:     Estimate $\hat{R}_{fair}(\boldsymbol{\theta}_c, \boldsymbol{\theta}_g) \approx \sum_{k=1}^{K} \left| \pi_k^{a=-1} - \pi_k^{a=1} \right|$
 6:     Evaluate $R_{cls}(\boldsymbol{\theta}_c, \boldsymbol{\theta}_g, \boldsymbol{\theta}_w)$ using Eq.(8)
 7:     Define $R_{total}$ using Eq.(10)
 8:     Primal Update $\boldsymbol{\theta} \leftarrow \text{Adam}(R_{cls} + \lambda_1 R_{inv} + \lambda_2 \hat{R}_{fair}, \boldsymbol{\theta}, \eta_1)$
 9:     Dual Update $\lambda_1 \leftarrow \max\left\{\left[\lambda_1 + \eta_2\left(R_{inv} - \epsilon_1\right)\right], 0\right\}$,
                    $\lambda_2 \leftarrow \max\left\{\left[\lambda_2 + \eta_3\left(\hat{R}_{fair} - \epsilon_2\right)\right], 0\right\}$
10: until convergence
11: procedure FairGMMs($Q, \boldsymbol{\theta}_c$)
12:     for each $a \in \{-1, 1\}$ do
13:         Define $\{\mathbf{c}_i^a\}_{i=1}^{N^a}$ by encoding $Q$ using $h_c$ and $\boldsymbol{\theta}_c$ with
            respect to the sensitive subgroup $a$
14:         repeat
15:             Estimate $\{\gamma_{k,i}^a\}_{i=1}^{N^a}$ using Eq.(3)
16:             Update $\boldsymbol{\mu}_k^a \leftarrow \frac{\sum_{i=1}^{N^a} \gamma_{k,i}^a \mathbf{c}_i^a}{\sum_{i=1}^{N^a} \gamma_{k,i}^a}$
17:             Update $\Sigma_k^a \leftarrow \frac{\sum_{i=1}^{N^a} \gamma_{k,i}^a (\mathbf{c}_i^a - \boldsymbol{\mu}_k^a)(\mathbf{c}_i^a - \boldsymbol{\mu}_k^a)^T}{\sum_{i=1}^{N^a} \gamma_{k,i}^a}$
18:             Update $\pi_k^a \leftarrow \begin{cases} \frac{\sum_{i=1}^{N^a} \gamma_{k,i}^a}{N^a + \lambda_2}, & \text{if } \pi_k^a \geq \pi_k^{-a} \\ \frac{\sum_{i=1}^{N^a} \gamma_{k,i}^a}{N^a - \lambda_2}, & \text{otherwise} \end{cases}$
19:         until convergence
20:     end for
21: end procedure
```

Finally, the fair loss R_{fair} is defined over the data batch with all sensitive attributes using Eq.(5),

$$R_{fair}(\boldsymbol{\theta}_c, \boldsymbol{\theta}_g) = \mathcal{L}_{fair}(Q, \boldsymbol{\theta}_c, \boldsymbol{\theta}_g) \tag{9}$$

Therefore the total loss is given

$$R_{total} = R_{cls} + \lambda_1 \cdot R_{inv} + \lambda_2 \cdot R_{fair} \tag{10}$$

where $\lambda_1, \lambda_2 > 0$ are Lagrangian multipliers.

4.4 An Effective Algorithm

We introduce an effective algorithm for FLAIR to implement the predictor f, as shown in Algorithm 1. Lines 2-3 represent the transformation model T, while lines 4-6 denote the fair representation learner g. In the g component, we employ $\hat{R}_{fair}$ as an approximation to R_{fair}, since the EM algorithm[22] in FairGMMs continuously estimates γ_k^a using $\pi_k^a, \forall k, a$. Parameters of $\boldsymbol{\theta}_g$ update are given in lines 15-18 of Algorithm 1. We optimize λ_1 and λ_2 in the R_{total} using the primal-dual algorithm, which is an effective tool for enforcing invariance [27]. The time complexity of Algorithm 1 is $O(M \times Q \times (N^{a=1} + N^{a=-1}))$, where M is the number of batches.

5 Experimental Settings

5.1 Datasets

`Rotated-Colored-MNIST` (`RCMNIST`) dataset is a synthetic image dataset generated from the MNIST dataset [16] by rotating and coloring the digits. The rotation angles $d \in \{0°,15°,30°,45°,60°,75°\}$ of the digits are used to partition different domains, while the color $a \in \{\text{red}, \text{green}\}$ of the digits is served as the sensitive attribute. A binary target label is created by grouping digits into $\{0, 1, 2, 3, 4\}$ and $\{5, 6, 7, 8, 9\}$. To investigate the robustness of FLAIR in the face of correlation shift, we controlled the correlation between label and color for each domain in the generation process of `RCMNIST`, setting them respectively to $\{0, 0.8, 0.5, 0.1, 0.3, 0.6\}$. The correlation for domain $d = 0°$ was set to 0, implying that higher accuracy leads to fairer results.

`New-York-Stop-and-Frisk` (`NYPD`) dataset [9] is a real-world tabular dataset containing stop, question, and frisk data from some suspects in five different cities. We selected the full-year data from 2011, which had the highest number of stops compared to any other year. We consider the cities $d \in${BROOKLYN, QUEENS, MANHATTAN, BRONX, STATEN IS} where suspects were sampled as domains. The suspects' gender $a \in$ {Male, Female} serves as the sensitive attribute, and whether a suspect was frisked is treated as the target label.

`FairFace` dataset [13] is a novel face image dataset containing 108,501 images labeled with race, gender, and age groups which is balanced on race. The dataset comprises face images from seven race group $d \in$ {White, Black, Latino/Hispanic, East Asian, Southeast Asian, Indian, Middle Eastern}. These race groups determine the domain to which an image belongs. Gender $a \in$ {Male, Female} is considered a sensitive attribute, and the binary target label is determined based on whether the age is greater than 60 years old.

5.2 Evaluation Metrics

Given input feature $X \in \mathcal{X}$, target label $Y \in \mathcal{Y} = \{0, 1\}$ and binary sensitive attribute $A \in \mathcal{A} = \{-1, 1\}$, we evaluate the algorithm's performance on the test dataset $\mathcal{D}_{te}$. We measure the DG performance of the algorithm using **Accuracy** and evaluate the algorithm fairness using the following metrics.

Demographic parity difference (Δ_{DP}) [6] is a type of *group fairness* metric. Its rationale is that the acceptance rate provided by the algorithm should be the same across all sensitive subgroups. It can be formalized as

$$\Delta_{DP} = \left| P(\hat{Y} = 1 | A = -1) - P(\hat{Y} = 1 | A = 1) \right|,$$

where $\hat{Y}$ is the predicted class label. The smaller the Δ_{DP}, the fairer the algorithm.

AUC for fairness (AUC_{fair}) [2] is a pairwise *group fairness* metric. Define a scoring function $q_\theta : \mathcal{X} \to \mathbb{R}$, where θ represents the model parameters. The AUC_{fair} of q_θ measures the probability

Table 1: Performance on RCMNIST (bold is the best, underline is the second best).

	Consisitency ↑ / Δ_{DP} ↓ / AUC$_{fair}$ ↓ / Accuracy ↑						
	0°	15°	30°	45°	60°	75°	Avg
ERM [32]	0.94 (0.03) / 0.04 (0.01) / 0.54 (0.01) / 92.02 (0.35)	0.95 (0.05) / 0.32 (0.04) / 0.67 (0.01) / **98.34 (0.17)**	0.95 (0.03) / 0.15 (0.01) / 0.56 (0.01) / 97.99 (0.34)	0.95 (0.04) / 0.35 (0.05) / 0.69 (0.01) / 98.34 (0.12)	0.95 (0.01) / 0.29 (0.02) / 0.68 (0.01) / 98.04 (0.18)	0.93 (0.01) / 0.17 (0.02) / 0.62 (0.02) / 94.60 (0.46)	0.946 / 0.221 / 0.626 / 96.55
IRM [1]	0.96 (0.01) / 0.04 (0.01) / 0.53 (0.01) / 90.67 (0.89)	0.95 (0.05) / 0.32 (0.03) / 0.67 (0.01) / 97.94 (0.25)	0.95 (0.02) / 0.15 (0.03) / 0.55 (0.01) / 97.65 (0.28)	0.96 (0.05) / 0.35 (0.01) / 0.69 (0.01) / 97.68 (0.42)	0.96 (0.01) / 0.28 (0.01) / 0.66 (0.01) / 97.11 (0.47)	0.93 (0.02) / 0.16 (0.02) / 0.61 (0.01) / 93.67 (0.30)	0.953 / 0.217 / 0.619 / 95.79
GDRO [29]	0.95 (0.01) / 0.04 (0.02) / 0.55 (0.01) / 93.00 (0.67)	0.95 (0.02) / 0.31 (0.05) / 0.66 (0.01) / 98.07 (0.33)	0.95 (0.04) / 0.16 (0.01) / 0.58 (0.01) / 97.84 (0.30)	0.95 (0.05) / 0.35 (0.01) / 0.71 (0.02) / 98.07 (0.30)	0.96 (0.01) / 0.29 (0.01) / 0.69 (0.01) / 97.88 (0.39)	0.93 (0.04) / 0.16 (0.01) / 0.61 (0.01) / 94.40 (0.41)	0.952 / 0.220 / 0.631 / 96.54
Mixup [37]	0.95 (0.01) / 0.04 (0.01) / 0.54 (0.01) / 93.27 (0.84)	0.95 (0.05) / 0.31 (0.05) / 0.66 (0.01) / 98.13 (0.20)	0.95 (0.05) / 0.16 (0.02) / 0.57 (0.01) / 98.26 (0.11)	0.95 (0.04) / 0.34 (0.03) / 0.69 (0.01) / 98.39 (0.22)	0.96 (0.03) / 0.29 (0.04) / 0.68 (0.01) / 97.94 (0.14)	0.93 (0.01) / 0.15 (0.01) / 0.59 (0.01) / 93.58 (0.61)	0.951 / 0.215 / 0.623 / 96.59
MLDG [18]	0.95 (0.01) / 0.04 (0.01) / 0.53 (0.01) / 92.37 (0.47)	0.95 (0.03) / 0.31 (0.03) / 0.65 (0.01) / 97.65 (0.18)	0.95 (0.05) / 0.16 (0.04) / 0.56 (0.01) / 98.07 (0.26)	0.95 (0.05) / 0.35 (0.01) / 0.70 (0.01) / 98.15 (0.07)	0.96 (0.03) / 0.28 (0.04) / 0.66 (0.01) / 97.59 (0.15)	0.94 (0.02) / 0.17 (0.04) / 0.62 (0.01) / 94.30 (0.36)	0.952 / 0.219 / 0.620 / 96.36
CORAL [31]	0.95 (0.01) / 0.04 (0.01) / 0.55 (0.01) / 93.81 (0.82)	0.96 (0.02) / 0.31 (0.03) / 0.67 (0.01) / 98.31 (0.44)	0.96 (0.03) / 0.16 (0.05) / 0.58 (0.01) / **98.49 (0.29)**	0.96 (0.05) / 0.35 (0.04) / 0.68 (0.01) / **98.63 (0.23)**	0.96 (0.05) / 0.29 (0.03) / 0.68 (0.01) / **98.33 (0.16)**	0.94 (0.01) / 0.16 (0.01) / 0.61 (0.02) / 95.43 (0.74)	0.954 / 0.221 / 0.628 / 97.17
DANN [8]	0.94 (0.02) / 0.04 (0.01) / 0.54 (0.01) / 91.24 (2.11)	0.93 (0.05) / 0.30 (0.02) / 0.63 (0.04) / 96.74 (0.27)	0.93 (0.02) / 0.14 (0.01) / 0.54 (0.03) / 96.84 (0.34)	0.93 (0.02) / 0.35 (0.01) / 0.70 (0.01) / 97.36 (0.26)	0.94 (0.04) / 0.29 (0.01) / 0.69 (0.01) / 97.03 (0.25)	0.90 (0.01) / 0.17 (0.01) / 0.62 (0.01) / 90.60 (1.13)	0.928 / 0.216 / 0.620 / 94.97
CDANN [19]	0.94 (0.01) / 0.04 (0.01) / 0.53 (0.01) / 91.08 (1.21)	0.93 (0.05) / 0.31 (0.02) / 0.66 (0.01) / 97.47 (0.32)	0.93 (0.01) / 0.15 (0.01) / 0.57 (0.02) / 96.57 (0.66)	0.93 (0.03) / 0.35 (0.01) / 0.69 (0.02) / 97.61 (0.40)	0.94 (0.02) / 0.29 (0.03) / 0.67 (0.01) / 97.60 (0.17)	0.90 (0.02) / 0.18 (0.02) / 0.62 (0.01) / 90.63 (1.67)	0.928 / 0.219 / 0.623 / 95.16
DDG [39]	**0.97 (0.01)** / **0.01 (0.01)** / **0.50 (0.05)** / **96.90 (0.11)**	0.96 (0.03) / 0.31 (0.04) / 0.65 (0.01) / 97.79 (0.05)	0.97 (0.02) / 0.16 (0.01) / 0.59 (0.03) / 97.42 (0.33)	0.97 (0.02) / 0.35 (0.01) / 0.69 (0.05) / 97.97 (0.05)	0.97 (0.03) / 0.28 (0.02) / 0.64 (0.05) / 97.81 (0.06)	0.95 (0.03) / 0.15 (0.01) / 0.58 (0.01) / **96.74 (0.13)**	0.963 / 0.209 / 0.609 / **97.44**
DIR [7]	0.73 (0.03) / 0.02 (0.05) / 0.52 (0.05) / 71.89 (0.21)	0.73 (0.03) / 0.18 (0.03) / 0.57 (0.05) / 72.61 (0.24)	0.72 (0.02) / 0.17 (0.04) / 0.56 (0.01) / 71.72 (0.11)	0.73 (0.04) / **0.22 (0.02)** / 0.57 (0.03) / 72.35 (0.19)	0.72 (0.04) / **0.21 (0.03)** / **0.56 (0.03)** / 70.85 (0.21)	0.73 (0.02) / 0.16 (0.05) / 0.57 (0.01) / 69.69 (0.14)	0.728 / 0.161 / 0.555 / 71.52
EIIL [4]	0.93 (0.01) / 0.14 (0.04) / 0.58 (0.01) / 82.00 (0.76)	0.96 (0.02) / 0.27 (0.03) / 0.63 (0.06) / 92.07 (0.18)	0.96 (0.04) / 0.14 (0.01) / 0.61 (0.01) / 92.17 (0.28)	0.97 (0.03) / 0.26 (0.02) / 0.62 (0.01) / 91.83 (0.38)	0.96 (0.02) / 0.27 (0.01) / 0.59 (0.01) / 93.09 (0.22)	0.96 (0.02) / 0.21 (0.02) / 0.61 (0.01) / 93.77 (0.10)	0.959 / 0.216 / 0.607 / 90.82
FVAE [25]	0.95 (0.02) / 0.07 (0.03) / 0.53 (0.03) / 91.44 (2.02)	0.96 (0.01) / 0.30 (0.02) / 0.59 (0.06) / 92.49 (1.42)	0.96 (0.06) / 0.18 (0.05) / 0.60 (0.04) / 91.69 (6.34)	0.97 (0.01) / 0.28 (0.04) / **0.56 (0.02)** / 92.85 (1.30)	0.97 (0.01) / 0.28 (0.01) / 0.67 (0.03) / 91.02 (1.25)	0.94 (0.02) / 0.21 (0.02) / 0.60 (0.03) / 91.34 (1.74)	0.958 / 0.220 / 0.592 / 91.80
FATDM [26]	0.94 (0.01) / **0.01 (0.01)** / 0.52 (0.02) / 94.02 (1.02)	0.95 (0.01) / 0.19 (0.01) / **0.55 (0.02)** / 90.65 (1.42)	0.94 (0.01) / 0.14 (0.02) / 0.55 (0.02) / 90.25 (1.36)	0.96 (0.04) / 0.25 (0.01) / 0.57 (0.02) / 92.90 (1.21)	0.95 (0.02) / 0.26 (0.03) / 0.57 (0.01) / 91.72 (1.32)	0.96 (0.01) / 0.14 (0.02) / 0.57 (0.03) / 91.11 (0.84)	0.953 / 0.165 / 0.555 / 91.78
FLAIR	0.97 (0.02) / 0.02 (0.01) / 0.52 (0.01) / 93.11 (1.23)	**0.99 (0.02)** / **0.18 (0.02)** / 0.56 (0.04) / 90.85 (1.56)	**0.99 (0.02)** / **0.12 (0.03)** / **0.54 (0.02)** / 91.77 (1.94)	**0.98 (0.02)** / 0.28 (0.02) / 0.56 (0.03) / 92.05 (2.34)	**0.98 (0.02)** / 0.24 (0.03) / 0.56 (0.04) / 91.95 (2.23)	**0.98 (0.01)** / **0.11 (0.03)** / **0.56 (0.04)** / 91.55 (1.02)	**0.980** / **0.157** / **0.552** / 91.88

of correctly ranking positive examples ahead of negative examples.

$$AUC_{fair}(q_\theta) = \frac{\sum_{X \in \mathcal{D}_{te}^{a=1}} \sum_{X' \in \mathcal{D}_{te}^{a=-1}} \mathbb{1}[q_\theta(X) > q_\theta(X')]}{N^{a=1} \times N^{a=-1}},$$

where $\mathbb{1}(\cdot)$ is an indicator function that returns 1 when the parameter is true and 0 otherwise. $\mathcal{D}_{te}$ is divided into $\mathcal{D}_{te}^{a=1}$ and $\mathcal{D}_{te}^{a=-1}$ based on A, which respectively contain $N^{a=1}$ and $N^{a=-1}$ samples. The value of AUC_{fair} ranges from 0 to 1, with a value closer to 0.5 indicating a fairer algorithm.

Consistency [38] is an *individual fairness* metric based on the Lipschitz condition [6]. Specifically, *Consistency* measures the distance between each individual and its k-nearest neighbors.

$$Consistency = 1 - \frac{1}{N}\sum_{i=1}^{N}\left|\hat{y}_i - \frac{1}{k}\sum_{j \in k\mathrm{NN}(\mathbf{x}_i)} \hat{y}_j\right|,$$

where N is the total number of samples in $\mathcal{D}_{te}$, $\hat{y}_i$ is the predicted class label for sample $\mathbf{x}_i$, and kNN$(\cdot)$[1] takes the features of sample $\mathbf{x}_i$ as input and returns the set of indices corresponding to its k-nearest neighbors in the feature space. A larger *Consistency* indicates a higher level of individual fairness.

5.3 Compared Methods

We validate the utility of FLAIR in handling Problem 1 using 13 methods. ERM [32], IRM [1], GDRO [29], Mixup [37], MLDG [18], CORAL [31], DANN [8], CDANN [19], and DDG [39] are DG methods without fairness consideration. Among them, DDG is a recently proposed method that focuses on learning invariant representations through disentanglement. DIR [7] is a classic group fairness algorithm. EIIL [4] and FVAE [25] can achieve both domain generalization under correlation shift and fairness. FATDM [26] is the latest work that explicitly focuses on both domain generalization under covariate shift and group fairness simultaneously.

6 Results

To evaluate the performance of FLAIR, we posed the following research questions from shallow to deep and answered them in Sections 6.1, 6.3 and 6.2.

- *Q1)* Can FLAIR effectively address Problem 1, or in other words, can FLAIR ensure both group fairness and individual fairness on unseen domains while maximizing DG performance?
- *Q2)* Does FLAIR exhibit a good trade-off between DG performance and fairness?
- *Q3)* What are the roles of the transformation model T and the fair representation learner g in FLAIR?
- *Q4)* How is R_{fair} ensuring algorithmic fairness in the learning process of FLAIR?

6.1 Overall Performance

The overall performance of FLAIR and its competing methods on three real-world datasets is presented in Table 1, 2 and 3, ↑ means

[1] Note that in [38], kNN$(\cdot)$ is applied to the full set of samples. To adapt it for DG task, here we apply it only to the set for the domain in which the samples are located.

Table 2: Performance on NYPD (bold is the best, underline is the second best).

	Consisitency ↑ / Δ_{DP} ↓ / AUC$_{fair}$ ↓ / Accuracy ↑					
	BROOKLYN	QUEENS	MANHATTAN	BRONX	STATEN IS	Avg
ERM [32]	0.92 (0.03) / 0.14 (0.01) / 0.60 (0.03) / **62.57 (0.15)**	0.92 (0.03) / 0.11 (0.01) / 0.58 (0.03) / 61.47 (0.15)	0.91 (0.03) / 0.13 (0.04) / 0.60 (0.03) / 60.60 (0.16)	0.90 (0.01) / 0.03 (0.03) / 0.55 (0.04) / 61.07 (0.46)	0.91 (0.03) / 0.15 (0.01) / 0.61 (0.01) / <u>67.02 (0.30)</u>	0.910 / 0.113 / 0.588 / 62.55
IRM [1]	0.93 (0.02) / 0.17 (0.01) / 0.62 (0.05) / <u>62.54 (0.07)</u>	0.92 (0.03) / 0.13 (0.01) / 0.60 (0.01) / 61.80 (0.38)	0.92 (0.01) / 0.15 (0.01) / 0.61 (0.01) / <u>61.10 (0.13)</u>	0.91 (0.04) / 0.06 (0.04) / 0.55 (0.02) / 59.84 (1.83)	0.91 (0.01) / 0.17 (0.01) / 0.62 (0.01) / 66.68 (0.16)	0.916 / 0.136 / 0.598 / 62.39
GDRO [29]	0.93 (0.01) / 0.14 (0.01) / 0.60 (0.04) / 62.10 (0.17)	0.92 (0.01) / 0.12 (0.01) / 0.59 (0.04) / 61.94 (0.30)	0.92 (0.01) / 0.15 (0.01) / 0.60 (0.01) / 60.50 (0.07)	0.91 (0.04) / 0.04 (0.03) / 0.53 (0.02) / 60.94 (1.73)	0.91 (0.04) / 0.15 (0.01) / 0.60 (0.01) / 66.48 (0.20)	0.914 / 0.121 / 0.585 / 62.39
Mixup [37]	0.92 (0.03) / 0.13 (0.01) / 0.59 (0.01) / 62.24 (0.30)	0.92 (0.01) / 0.10 (0.01) / 0.58 (0.01) / <u>62.34 (0.98)</u>	0.92 (0.01) / 0.13 (0.01) / 0.60 (0.01) / 60.17 (0.38)	0.90 (0.02) / 0.07 (0.02) / 0.56 (0.01) / 61.30 (1.96)	0.91 (0.02) / 0.14 (0.01) / 0.59 (0.05) / 66.25 (0.85)	0.914 / 0.113 / 0.583 / 62.46
MLDG [18]	0.93 (0.03) / 0.14 (0.01) / 0.60 (0.02) / 62.54 (0.13)	0.92 (0.04) / 0.11 (0.01) / 0.58 (0.01) / 61.45 (0.23)	0.92 (0.04) / 0.13 (0.05) / 0.60 (0.05) / 60.53 (0.18)	0.91 (0.05) / 0.03 (0.01) / 0.53 (0.02) / 60.94 (2.43)	0.91 (0.04) / 0.15 (0.04) / 0.61 (0.03) / 66.94 (0.25)	0.916 / 0.113 / 0.585 / 62.48
CORAL [31]	0.93 (0.02) / 0.15 (0.01) / 0.61 (0.01) / 62.38 (0.10)	0.92 (0.01) / 0.11 (0.04) / 0.58 (0.01) / 61.51 (0.40)	0.91 (0.02) / 0.13 (0.01) / 0.60 (0.01) / 60.61 (0.15)	0.91 (0.01) / 0.04 (0.03) / 0.54 (0.02) / 61.52 (3.13)	0.91 (0.02) / 0.15 (0.01) / 0.60 (0.02) / **67.08 (0.21)**	0.917 / 0.114 / 0.586 / <u>62.62</u>
DANN [8]	0.92 (0.01) / 0.15 (0.02) / 0.61 (0.01) / 61.78 (0.32)	0.92 (0.02) / 0.11 (0.01) / 0.58 (0.01) / 61.06 (1.33)	0.91 (0.05) / 0.15 (0.02) / 0.60 (0.01) / 60.51 (0.57)	0.88 (0.03) / 0.10 (0.01) / 0.56 (0.02) / 58.32 (1.28)	0.91 (0.03) / 0.14 (0.01) / 0.60 (0.01) / 65.62 (0.18)	0.910 / 0.130 / 0.591 / 61.46
CDANN [19]	0.93 (0.05) / 0.15 (0.01) / 0.60 (0.01) / 62.07 (0.27)	0.92 (0.02) / 0.11 (0.01) / 0.58 (0.01) / 61.28 (1.56)	0.91 (0.04) / 0.15 (0.01) / 0.61 (0.01) / 60.59 (0.36)	0.90 (0.02) / 0.09 (0.03) / 0.56 (0.02) / 61.26 (1.25)	0.91 (0.05) / 0.17 (0.01) / 0.61 (0.01) / 66.07 (0.59)	0.914 / 0.132 / 0.594 / 62.25
DDG [39]	0.94 (0.02) / 0.14 (0.01) / 0.60 (0.02) / 62.46 (0.11)	0.94 (0.02) / 0.11 (0.01) / 0.58 (0.04) / **62.45 (0.13)**	0.94 (0.03) / 0.13 (0.01) / 0.60 (0.04) / **61.11 (0.29)**	0.93 (0.03) / 0.02 (0.02) / <u>0.53 (0.01)</u> / **64.91 (0.57)**	0.93 (0.04) / 0.15 (0.01) / 0.60 (0.01) / 66.46 (0.22)	0.935 / 0.109 / 0.582 / **63.48**
DIR [7]	0.87 (0.03) / 0.14 (0.01) / 0.58 (0.05) / 57.23 (0.04)	0.89 (0.01) / 0.10 (0.04) / 0.58 (0.05) / 55.80 (0.23)	0.88 (0.02) / 0.11 (0.02) / 0.57 (0.02) / 56.19 (0.11)	0.90 (0.04) / 0.08 (0.02) / 0.58 (0.03) / 54.25 (0.17)	0.89 (0.03) / **0.11 (0.02)** / 0.56 (0.01) / 55.19 (0.11)	0.883 / 0.107 / 0.577 / 55.73
EIIL [4]	0.94 (0.03) / 0.11 (0.01) / 0.59 (0.01) / 59.92 (1.16)	0.94 (0.02) / 0.10 (0.01) / 0.58 (0.01) / 56.06 (0.24)	0.93 (0.05) / **0.04 (0.01)** / **0.55 (0.01)** / 53.08 (0.98)	0.92 (0.04) / 0.03 (0.02) / <u>0.53 (0.01)</u> / 61.02 (1.14)	<u>0.94 (0.02)</u> / 0.13 (0.01) / **0.55 (0.01)** / 56.69 (0.98)	0.933 / <u>0.080</u> / <u>0.561</u> / 57.35
FVAE [25]	<u>0.95 (0.01)</u> / 0.12 (0.01) / 0.61 (0.01) / 58.78 (0.88)	**0.96 (0.02)** / 0.13 (0.01) / 0.58 (0.01) / 58.76 (3.17)	<u>0.94 (0.01)</u> / 0.13 (0.01) / 0.61 (0.03) / 60.63 (2.95)	0.93 (0.04) / 0.04 (0.01) / 0.54 (0.01) / 61.08 (1.16)	0.93 (0.02) / 0.16 (0.01) / 0.56 (0.03) / 63.96 (1.58)	<u>0.941</u> / 0.115 / 0.578 / 60.64
FATDM [26]	0.93 (0.01) / **0.09 (0.01)** / <u>0.58 (0.02)</u> / 60.13 (1.10)	0.93 (0.02) / <u>0.05 (0.02)</u> / **0.56 (0.01)** / 58.48 (0.57)	<u>0.94 (0.01)</u> / 0.12 (0.01) / 0.57 (0.01) / 57.02 (0.63)	<u>0.94 (0.02)</u> / **0.01 (0.02)** / 0.54 (0.01) / 62.57 (0.59)	0.93 (0.05) / 0.14 (0.01) / 0.57 (0.02) / 62.80 (1.83)	0.931 / 0.082 / 0.566 / 60.20
FLAIR	**0.96 (0.01)** / <u>0.10 (0.02)</u> / **0.58 (0.01)** / 58.08 (1.08)	<u>0.96 (0.04)</u> / **0.03 (0.02)** / <u>0.57 (0.01)</u> / 60.82 (0.55)	**0.95 (0.02)** / <u>0.10 (0.01)</u> / <u>0.56 (0.02)</u> / 58.14 (0.44)	**0.94 (0.01)** / <u>0.02 (0.02)</u> / **0.52 (0.01)** / <u>63.87 (1.14)</u>	**0.95 (0.05)** / <u>0.12 (0.01)</u> / <u>0.55 (0.03)</u> / 62.63 (1.06)	**0.955** / **0.073** / **0.560** / 60.71

higher is better, ↓ means lower is better. Each experiment was conducted five times and the average results were recorded, with standard deviations reported in parentheses.

Fairness Evaluation. Focus on the average of each fairness metric across all domains, FLAIR almost achieves the best performance on all three datasets. Excluding DIR, which is not competitive due to its poor DG performance, FLAIR consistently ranks as either the fairest or the second fairest in each domain. This indicates its relative stability in achieving fairness across various domains compared to competing methods. All of the above analyses shows that FLAIR is able to achieve both individual fairness and group fairness on unseen domains with state-of-the-art results.

DG Evaluation Considering Trade-off. Considering the accuracy-fairness trade-off, we aim to enhance DG performance while simultaneously ensuring algorithmic fairness. From this perspective, we notice that (i) methods solely focusing on DG cannot ensure algorithmic fairness effectively. (ii) Although lower than the above methods, the performance of DG for FLAIR is still competitive, and it outperforms other competing algorithms that also focus on fairness. (iii) On the FairFace dataset, FLAIR ensures the best fairness while its DG performance is second only to DDG. This is because the transformation model allows FLAIR to learn better domain-invariant representations when dealing with relatively complex data (facial photos) and types of environments.

Overall, FLAIR ensures fairness on both tabular and image data while maintaining strong DG capabilities. It can learn a fairness-aware domain-invariant predictor to effectively address Problem 1. The success of FLAIR on all three datasets, particularly RCMNIST, also demonstrates that our approach works effectively when dealing with DG problems involving covariate shift and correlation shift.

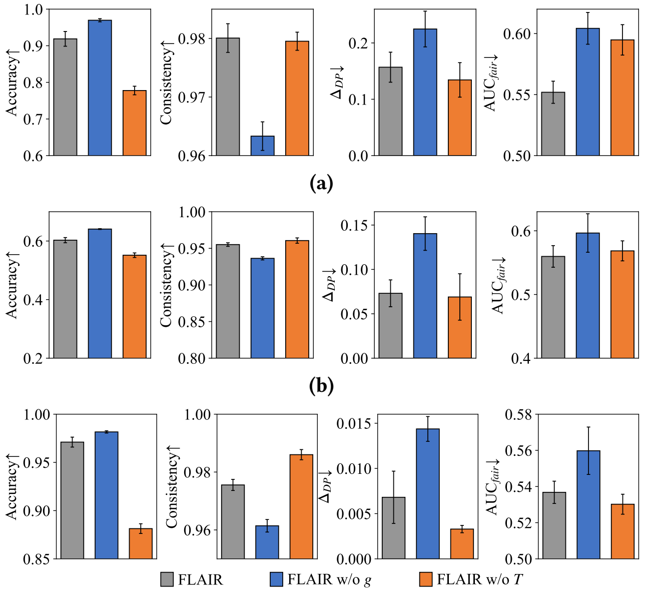

(a)

(b)

(c)

Figure 3: Ablation study over four metrics for FLAIR and its two variants on (a) RCMNIST, (b) NYPD and (c) FairFace datasets. Results are averaged across all domains.

Table 3: Performance on `FairFace` (bold is the best, underline is the second best).

	Consisitency ↑ / Δ_{DP} ↓ / AUC$_{fair}$ ↓ / Accuracy ↑			
	White	Black	Latino/Hispanic	East Asian
ERM [32]	0.95 (0.02) / 0.05 (0.02) / 0.57 (0.01) / 92.97 (3.04)	0.95 (0.01) / 0.03 (0.01) / 0.58 (0.01) / 91.31 (2.28)	0.96 (0.04) / 0.02 (0.01) / 0.57 (0.02) / 95.33 (1.51)	0.96 (0.03) / 0.02 (0.01) / 0.60 (0.01) / 96.71 (0.28)
IRM [1]	0.95 (0.01) / 0.05 (0.01) / 0.57 (0.01) / 93.26 (1.17)	0.96 (0.01) / 0.02 (0.01) / 0.57 (0.01) / 92.94 (1.01)	0.96 (0.03) / 0.03 (0.02) / 0.56 (0.03) / 94.85 (2.27)	0.95 (0.01) / 0.03 (0.01) / 0.60 (0.01) / 95.23 (1.26)
GDRO [29]	0.95 (0.01) / 0.06 (0.01) / 0.57 (0.01) / 91.94 (0.47)	0.96 (0.01) / 0.02 (0.01) / 0.58 (0.01) / 92.67 (1.59)	0.96 (0.01) / 0.01 (0.02) / 0.57 (0.01) / 96.14 (0.69)	0.96 (0.01) / 0.02 (0.01) / 0.61 (0.01) / 96.63 (0.30)
Mixup [37]	0.95 (0.04) / 0.05 (0.01) / 0.55 (0.05) / 92.29 (2.26)	0.95 (0.01) / 0.03 (0.01) / 0.53 (0.01) / 92.49 (2.20)	0.96 (0.03) / 0.02 (0.03) / 0.54 (0.03) / 95.42 (1.02)	0.96 (0.01) / 0.03 (0.01) / 0.55 (0.02) / 96.09 (1.43)
MLDG [18]	0.95 (0.05) / 0.05 (0.01) / 0.58 (0.01) / 93.71 (0.41)	0.95 (0.04) / 0.02 (0.01) / 0.58 (0.01) / 93.21 (0.40)	0.96 (0.03) / 0.02 (0.02) / 0.58 (0.01) / 95.64 (0.93)	0.95 (0.03) / 0.02 (0.01) / 0.59 (0.02) / 96.34 (0.84)
CORAL [31]	0.95 (0.05) / 0.07 (0.02) / 0.57 (0.01) / 91.99 (2.14)	0.95 (0.04) / 0.05 (0.01) / 0.57 (0.01) / 89.44 (2.35)	0.95 (0.05) / 0.04 (0.01) / 0.56 (0.01) / 93.97 (0.57)	0.95 (0.02) / 0.04 (0.01) / 0.57 (0.03) / 94.84 (0.99)
DANN [8]	0.93 (0.04) / 0.11 (0.01) / 0.59 (0.01) / 80.72 (2.23)	0.92 (0.01) / 0.09 (0.01) / 0.58 (0.01) / 74.07 (1.65)	0.93 (0.04) / 0.09 (0.02) / 0.61 (0.04) / 87.17 (2.48)	0.92 (0.02) / 0.10 (0.02) / 0.60 (0.01) / 85.42 (3.67)
CDANN [19]	0.91 (0.05) / 0.12 (0.02) / 0.59 (0.01) / 76.13 (2.65)	0.91 (0.03) / 0.08 (0.01) / 0.58 (0.01) / 76.43 (2.09)	0.92 (0.01) / 0.06 (0.01) / 0.60 (0.01) / 91.03 (1.42)	0.92 (0.02) / 0.08 (0.02) / 0.60 (0.01) / 89.09 (2.69)
DDG [39]	0.95 (0.04) / 0.04 (0.04) / 0.56 (0.01) / 96.25 (0.64)	0.96 (0.05) / 0.03 (0.01) / 0.55 (0.01) / 97.26 (0.60)	0.97 (0.03) / 0.01 (0.01) / 0.55 (0.02) / 98.15 (0.52)	0.96 (0.03) / 0.02 (0.01) / 0.59 (0.01) / **98.37 (0.63)**
DIR [7]	0.74 (0.04) / 0.02 (0.03) / **0.52 (0.05)** / 76.14 (0.11)	0.75 (0.04) / 0.03 (0.01) / **0.52 (0.03)** / 76.31 (0.17)	0.75 (0.04) / 0.03 (0.03) / **0.52 (0.02)** / 76.65 (0.19)	0.75 (0.01) / 0.03 (0.01) / **0.52 (0.04)** / 77.42 (0.21)
EIIL [4]	0.96 (0.01) / **0.01 (0.00)** / 0.55 (0.01) / 89.92 (0.12)	0.96 (0.05) / **0.00 (0.00)** / 0.59 (0.01) / 96.79 (0.11)	0.97 (0.05) / 0.11 (0.03) / 0.55 (0.01) / 83.76 (0.57)	0.97 (0.05) / 0.07 (0.01) / 0.60 (0.03) / 86.35 (1.87)
FVAE [25]	0.94 (0.01) / 0.05 (0.04) / 0.54 (0.02) / 90.36 (1.05)	0.91 (0.02) / 0.03 (0.01) / 0.57 (0.04) / 89.63 (2.22)	0.97 (0.02) / 0.03 (0.01) / 0.55 (0.01) / 93.30 (0.97)	**0.98 (0.01)** / 0.05 (0.01) / 0.57 (0.02) / 91.44 (1.58)
FATDM [26]	0.95 (0.01) / 0.02 (0.02) / 0.53 (0.03) / 96.23 (1.11)	0.96 (0.01) / 0.02 (0.02) / 0.54 (0.01) / 95.82 (0.13)	0.95 (0.01) / 0.02 (0.04) / 0.55 (0.02) / 95.38 (0.29)	0.95 (0.03) / 0.01 (0.01) / 0.55 (0.04) / 96.31 (0.35)
FLAIR	**0.98 (0.01)** / 0.02 (0.01) / 0.57 (0.01) / **96.56 (0.76)**	**0.98 (0.01)** / 0.01 (0.00) / 0.53 (0.01) / **97.60 (0.13)**	**0.98 (0.01)** / **0.00 (0.00)** / 0.54 (0.01) / **98.31 (0.30)**	0.97 (0.02) / **0.00 (0.00)** / 0.55 (0.01) / 97.36 (0.28)

	Southeast Asian	Indian	Middle Eastern	Avg
ERM [32]	0.96 (0.03) / 0.01 (0.01) / 0.56 (0.01) / 94.42 (0.29)	0.94 (0.04) / 0.01 (0.03) / 0.53 (0.02) / 94.66 (0.32)	0.95 (0.02) / 0.04 (0.01) / 0.57 (0.02) / 93.42 (1.85)	0.952 / 0.026 / 0.568 / 94.12
IRM [1]	0.96 (0.05) / 0.01 (0.01) / 0.56 (0.01) / 94.56 (0.41)	0.93 (0.04) / 0.02 (0.02) / 0.54 (0.02) / 94.27 (0.29)	0.94 (0.04) / 0.04 (0.01) / 0.56 (0.01) / 93.95 (1.37)	0.950 / 0.029 / 0.566 / 94.15
GDRO [29]	0.96 (0.01) / 0.02 (0.01) / 0.57 (0.02) / 94.26 (0.47)	0.94 (0.02) / 0.02 (0.01) / 0.53 (0.01) / 93.99 (0.79)	0.95 (0.03) / 0.04 (0.01) / 0.57 (0.01) / 93.87 (0.47)	0.954 / 0.027 / 0.570 / 94.21
Mixup [37]	0.96 (0.04) / 0.01 (0.02) / 0.51 (0.01) / 94.55 (0.28)	0.94 (0.01) / 0.03 (0.01) / 0.53 (0.01) / 93.76 (0.46)	0.95 (0.05) / 0.04 (0.01) / 0.55 (0.02) / 93.83 (0.44)	0.953 / 0.029 / 0.538 / 94.06
MLDG [18]	0.96 (0.05) / 0.01 (0.02) / 0.56 (0.02) / 94.62 (0.16)	0.93 (0.03) / 0.02 (0.02) / 0.56 (0.02) / 94.68 (0.37)	0.95 (0.03) / 0.03 (0.01) / 0.58 (0.01) / 94.57 (0.20)	0.952 / 0.023 / 0.577 / 94.68
CORAL [31]	0.96 (0.05) / 0.02 (0.01) / 0.54 (0.02) / 93.96 (0.74)	0.93 (0.05) / 0.03 (0.01) / 0.54 (0.02) / 93.78 (0.45)	0.94 (0.02) / 0.05 (0.01) / 0.56 (0.02) / 92.56 (0.73)	0.949 / 0.043 / 0.558 / 92.93
DANN [8]	0.91 (0.05) / 0.04 (0.01) / 0.56 (0.01) / 86.96 (1.54)	0.90 (0.04) / 0.07 (0.01) / 0.58 (0.02) / 88.35 (1.85)	0.92 (0.02) / 0.09 (0.02) / 0.60 (0.02) / 84.68 (3.25)	0.918 / 0.082 / 0.590 / 83.91
CDANN [19]	0.93 (0.05) / 0.04 (0.02) / 0.55 (0.01) / 84.56 (2.98)	0.91 (0.02) / 0.06 (0.03) / 0.56 (0.03) / 88.91 (3.54)	0.93 (0.02) / 0.05 (0.04) / 0.58 (0.01) / 86.14 (5.08)	0.918 / 0.070 / 0.581 / 84.61
DDG [39]	0.97 (0.03) / 0.01 (0.02) / 0.54 (0.01) / **97.98 (0.21)**	0.94 (0.04) / 0.01 (0.01) / 0.54 (0.02) / **97.29 (0.46)**	0.95 (0.01) / 0.04 (0.04) / 0.55 (0.02) / **97.13 (0.68)**	0.959 / 0.023 / 0.554 / **97.49**
DIR [7]	0.75 (0.03) / 0.03 (0.04) / 0.52 (0.02) / 75.46 (0.20)	0.74 (0.05) / 0.03 (0.01) / **0.52 (0.03)** / 74.55 (0.31)	0.75 (0.01) / 0.03 (0.03) / **0.52 (0.05)** / 68.14 (4.08)	0.748 / 0.027 / **0.521** / 74.95
EIIL [4]	0.97 (0.01) / 0.03 (0.01) / 0.54 (0.03) / 85.90 (0.82)	0.96 (0.02) / 0.04 (0.01) / 0.55 (0.01) / 88.96 (0.57)	0.96 (0.02) / 0.04 (0.02) / 0.56 (0.01) / 89.65 (0.26)	0.966 / 0.044 / 0.561 / 88.76
FVAE [25]	0.95 (0.01) / 0.03 (0.01) / 0.52 (0.01) / 90.23 (1.43)	0.96 (0.04) / 0.04 (0.01) / 0.54 (0.01) / 88.48 (1.18)	0.96 (0.01) / 0.06 (0.01) / 0.55 (0.02) / 86.80 (2.15)	0.954 / 0.041 / 0.550 / 90.04
FATDM [26]	0.95 (0.01) / 0.01 (0.01) / 0.53 (0.02) / 94.21 (1.45)	0.95 (0.01) / 0.01 (0.05) / 0.54 (0.03) / 94.52 (1.09)	0.95 (0.05) / 0.02 (0.01) / 0.54 (0.01) / 94.01 (0.58)	0.954 / 0.017 / 0.539 / 95.21
FLAIR	**0.98 (0.01)** / **0.00 (0.00)** / **0.51 (0.01)** / 96.75 (1.12)	**0.98 (0.01)** / **0.00 (0.00)** / 0.53 (0.01) / 96.87 (0.12)	**0.97 (0.02)** / **0.02 (0.00)** / 0.54 (0.01) / 96.28 (0.89)	**0.976** / **0.007** / 0.537 / 97.10

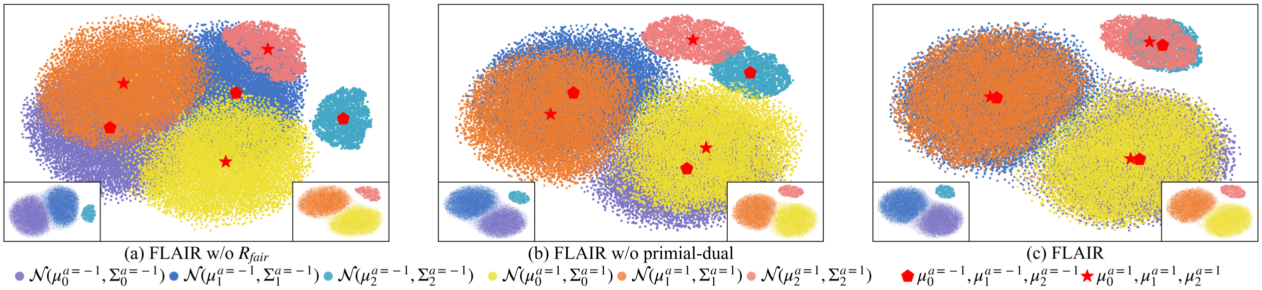
(a) FLAIR w/o R_{fair}

(b) FLAIR w/o primial-dual

(c) FLAIR

Figure 4: t-SNE visualization of the representations learned by (c) FLAIR and its variants (a) FLAIR w/o R_{fair} and (b) FLAIR w/o primal-dual on `RCMNIST` dataset. The main parts of (a)-(c) simultaneously visualize representations of two sensitive subgroups in the same latent space C, while the bottom-left ($a = -1$) and bottom-right ($a = 1$) visualize each group separately.

6.2 Ablation Study

To understand the roles of the transformation model T and the fair representation learner g in learning a fairness-aware domain invariant predictor, we constructed two different variants of FLAIR for experimentation. They are: (i) FLAIR *w/o* g: remove g, i.e., learn a predictor $f_{v1} = h_s \circ \omega$. (ii) FLAIR *w/o* T: replace T with a standard featurizer $h : \mathcal{X} \rightarrow \mathcal{X}' \subseteq \mathbb{R}^{d'}$ and modify the corresponding input and output dimensions of g and ω, i.e., learn a predictor $f_{v2} = h \circ g \circ \omega$. The results of ablation study for FLAIR and its two variants on three dataset are shown in Figure 3 (a), (b) and (c).

By comparing FLAIR with its variant FLAIR w/o g, we can see that the representations obtained by T exhibit strong domain invariance but do not ensure fairness. Additionally, the improvement of FLAIR on all three fairness metrics suggests that g can simultaneously enhance individual and group fairness. The difference between the results of them further validates the accuracy-fairness trade-off .

Contrasting FLAIR with its variant FLAIR w/o T further highlights the DG utility of T. At the same time, it's evident that while g focuses only on fairness, it doesn't necessarily result in fairer outcomes. The reason for this is that the fair representation obtained solely through g lacks domain invariance. As a result, it cannot handle covariate shift and correlation shift when generalizing to unseen domains.

The Utility of R_{fair} To understand how the critical component R_{fair} in g promotes algorithmic fairness, we created two new variants of FLAIR. They are (i) FLAIR w/o R_{fair}: removing R_{fair} from g and (ii) FLAIR w/o *primal-dual*: replacing the primal-dual updates

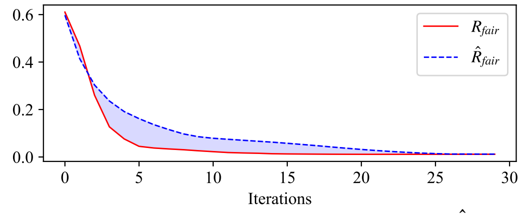

Figure 5: The convergence curves of R_{fair} and $\hat{R}_{fair}$ during training. Both of them converge after 30 iterations.

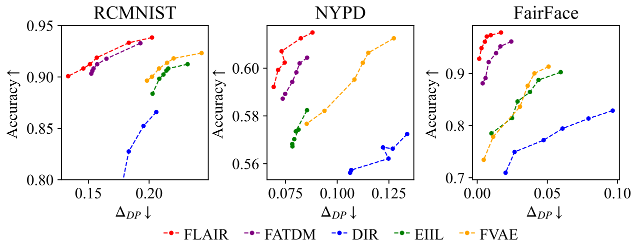

Figure 6: Accuracy-fairness trade-off across different methods by various $\lambda_2 \in \{0.05, 0.1, 0.5, 1, 2, 5\}$. The upper left indicates a better trade-off.

with fixed parameters λ_2. Figure 4 shows the visualization of the fair content representations $\{\tilde{\mathbf{c}}_i^a\}_{i=1}^{N^a}$ obtained by g and its two variants on RCMNIST, organized by the respective sensitive subgroups.

The transition from (a) to (b) and (c) clearly shows that during optimization R_{fair} brings the representations of the two sensitive subgroups closer in the latent space, ensuring that similar individuals from different groups get more similar representations. Additionally, the clustering of each sensitive subgroup can bring closer the distances between similar individuals within the same group. Combining above two points, R_{fair} enables FLAIR to achieve a strong individual fairness effect. At the same time, R_{fair} enforces statistical parity between sensitive subgroups, reducing the distances between corresponding prototypes of different groups. This also ensures that FLAIR achieves group fairness. The transition from (b) to (c) shows that optimizing through the primal-dual algorithm is able to achieve better algorithmic fairness performance.

The convergence curves for both R_{fair} and $\hat{R}_{fair}$ during training are shown in Figure 5. Since the prior π updates are not fully synchronized with the posterior γ updates (as seen in line 19 of Algorithm 1), a gap (indicated by the light blue area) exists between the two curves. However, their convergence trends are consistent, indicating that during training, $\hat{R}_{fair}$ can successfully approximate R_{fair} and does not affect the successful convergence of $\mathcal{L}_{gmm}$.

6.3 Sensitive Analysis

Accuracy-fairness Trade-off. To assess the trade-off performance of FLAIR, we obtained different group fairness and DG results of FLAIR by controlling the value of λ_2 (larger λ_2 implies FLAIR focuses more on algorithmic fairness). We compare the results with other fairness-aware methods, as shown in Figure 6 for all three datasets. It can be seen that the curve of the results obtained by FLAIR under different fairness levels is positioned in the upper-left corner among all methods. This indicates that FLAIR, while ensuring the best fairness performance, also maintains comparable domain generalization performance, achieving the best accuracy-fairness trade-off. Moreover, we observe that FLAIR achieves excellent fairness performance with comparable accuracy across all three datasets when $\lambda_2 = 0.5$. Therefore, we adopt this setting for all three datasets.

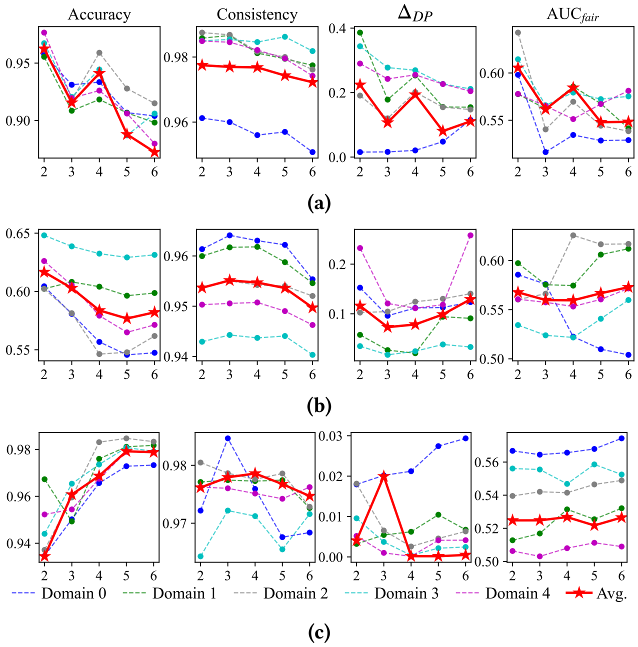

Figure 7: Performance of FLAIR on each domain and the average performance across different values of K on (a) RCMNIST, (b) NYPD and (c) FairFace datasets. The x-axis is the values of K ranging from 2 to 6.

Number of Prototypes. To determine the number of prototypes K in g, we conducted a sensitivity analysis of K. The experimental results on three datasets with fixed other parameters and varying values of K from 2 to 6 are shown in Figure 7. The number of prototypes we ultimately selected on the three datasets is 3, 3 and 4. Because at these values, FLAIR had the highest average ranking across the four metrics as well as the best accuracy-fairness trade-off.

7 Conclusion

In this paper, we introduce a novel approach to fairness-aware learning that tackles the challenges of generalization from observed training domains to unseen testing domains. In our pursuit of learning a fairness-aware invariant predictor across domains, we assert the existence of an underlying transformation model that can transform instances from one domain to another. To ensure prediction with fairness between sensitive subgroups, we present a fair representation approach, wherein latent content factors encoded from the transformation model are reconstructed while minimizing sensitive information. We present a practical and tractable algorithm. Exhaustive empirical studies showcase the algorithm's effectiveness through rigorous comparisons with state-of-the-art baselines.

Acknowledgments

This work is supported by the NSFC program (No. 62272338).

References

[1] Martin Arjovsky, Léon Bottou, Ishaan Gulrajani, and David Lopez-Paz. 2019. Invariant risk minimization. *arXiv preprint arXiv:1907.02893* (2019).

[2] Toon Calders, Asim Karim, Faisal Kamiran, Wasif Ali, and Xiangliang Zhang. 2013. Controlling attribute effect in linear regression. In *2013 IEEE 13th international conference on data mining*. IEEE, 71–80.

[3] Irene Chen, Fredrik D Johansson, and David Sontag. 2018. Why is my classifier discriminatory? *Advances in neural information processing systems* 31 (2018).

[4] Elliot Creager, Jörn-Henrik Jacobsen, and Richard Zemel. 2021. Environment inference for invariant learning. In *International Conference on Machine Learning*. PMLR, 2189–2200.

[5] Jacob Devlin, Ming-Wei Chang, Kenton Lee, and Kristina Toutanova. 2018. Bert: Pre-training of deep bidirectional transformers for language understanding. *arXiv preprint arXiv:1810.04805* (2018).

[6] Cynthia Dwork, Moritz Hardt, Toniann Pitassi, Omer Reingold, and Richard Zemel. 2012. Fairness through awareness. In *Proceedings of the 3rd innovations in theoretical computer science conference*. 214–226.

[7] Michael Feldman, Sorelle A Friedler, John Moeller, Carlos Scheidegger, and Suresh Venkatasubramanian. 2015. Certifying and removing disparate impact. In *proceedings of the 21th ACM SIGKDD international conference on knowledge discovery and data mining*. 259–268.

[8] Yaroslav Ganin, Evgeniya Ustinova, Hana Ajakan, Pascal Germain, Hugo Larochelle, François Laviolette, Mario Marchand, and Victor Lempitsky. 2016. Domain-adversarial training of neural networks. *The journal of machine learning research* 17, 1 (2016), 2096–2030.

[9] Sharad Goel, Justin M Rao, and Ravi Shroff. 2016. Precinct or prejudice? Understanding racial disparities in New York City's stop-and-frisk policy. (2016).

[10] Shishuai Hu, Zehui Liao, Jianpeng Zhang, and Yong Xia. 2022. Domain and content adaptive convolution based multi-source domain generalization for medical image segmentation. *IEEE Transactions on Medical Imaging* 42, 1 (2022), 233–244.

[11] Xin Jin, Cuiling Lan, Wenjun Zeng, and Zhibo Chen. 2020. Feature alignment and restoration for domain generalization and adaptation. *arXiv preprint arXiv:2006.12009* (2020).

[12] Jian Kang and Hanghang Tong. 2021. Fair graph mining. In *Proceedings of the 30th ACM International Conference on Information & Knowledge Management*. 4849–4852.

[13] Kimmo Karkkainen and Jungseock Joo. 2021. Fairface: Face attribute dataset for balanced race, gender, and age for bias measurement and mitigation. In *Proceedings of the IEEE/CVF winter conference on applications of computer vision*. 1548–1558.

[14] Alex Krizhevsky, Ilya Sutskever, and Geoffrey E Hinton. 2012. Imagenet classification with deep convolutional neural networks. *Advances in neural information processing systems* 25 (2012).

[15] Preethi Lahoti, Krishna P Gummadi, and Gerhard Weikum. 2019. ifair: Learning individually fair data representations for algorithmic decision making. In *2019 ieee 35th international conference on data engineering (icde)*. IEEE, 1334–1345.

[16] Yann LeCun, Léon Bottou, Yoshua Bengio, and Patrick Haffner. 1998. Gradient-based learning applied to document recognition. *Proc. IEEE* 86, 11 (1998), 2278–2324.

[17] Dong Li, Wenjun Wang, Minglai Shao, and Chen Zhao. 2023. Contrastive Representation Learning Based on Multiple Node-centered Subgraphs. In *Proceedings of the 32nd ACM International Conference on Information and Knowledge Management*. 1338–1347.

[18] Da Li, Yongxin Yang, Yi-Zhe Song, and Timothy Hospedales. 2018. Learning to generalize: Meta-learning for domain generalization. In *Proceedings of the AAAI conference on artificial intelligence*, Vol. 32.

[19] Ya Li, Xinmei Tian, Mingming Gong, Yajing Liu, Tongliang Liu, Kun Zhang, and Dacheng Tao. 2018. Deep domain generalization via conditional invariant adversarial networks. In *Proceedings of the European conference on computer vision (ECCV)*. 624–639.

[20] Yujie Lin, Dong Li, Chen Zhao, Xintao Wu, Qin Tian, and Minglai Shao. 2024. Supervised Algorithmic Fairness in Distribution Shifts: A Survey. *arXiv preprint arXiv:2402.01327* (2024).

[21] Michael Lohaus, Michael Perrot, and Ulrike Von Luxburg. 2020. Too relaxed to be fair. In *International Conference on Machine Learning*. PMLR, 6360–6369.

[22] Geoffrey J McLachlan and Thriyambakam Krishnan. 2007. *The EM algorithm and extensions*. John Wiley & Sons.

[23] Ninareh Mehrabi, Fred Morstatter, Nripsuta Saxena, Kristina Lerman, and Aram Galstyan. 2021. A survey on bias and fairness in machine learning. *ACM computing surveys (CSUR)* 54, 6 (2021), 1–35.

[24] Aditya Krishna Menon and Robert C Williamson. 2018. The cost of fairness in binary classification. In *Conference on Fairness, accountability and transparency*. PMLR, 107–118.

[25] Changdae Oh, Heeji Won, Junhyuk So, Taero Kim, Yewon Kim, Hosik Choi, and Kyungwoo Song. 2022. Learning fair representation via distributional contrastive disentanglement. In *Proceedings of the 28th ACM SIGKDD Conference on Knowledge Discovery and Data Mining*. 1295–1305.

[26] Thai-Hoang Pham, Xueru Zhang, and Ping Zhang. 2023. Fairness and accuracy under domain generalization. *arXiv preprint arXiv:2301.13323* (2023).

[27] Alexander Robey, George J Pappas, and Hamed Hassani. 2021. Model-based domain generalization. *Advances in Neural Information Processing Systems* 34 (2021), 20210–20229.

[28] Yuji Roh, Kangwook Lee, Steven Euijong Whang, and Changho Suh. 2023. Improving fair training under correlation shifts. In *International Conference on Machine Learning*. PMLR, 29179–29209.

[29] Shiori Sagawa, Pang Wei Koh, Tatsunori B Hashimoto, and Percy Liang. 2019. Distributionally robust neural networks for group shifts: On the importance of regularization for worst-case generalization. *arXiv preprint arXiv:1911.08731* (2019).

[30] Hidetoshi Shimodaira. 2000. Improving predictive inference under covariate shift by weighting the log-likelihood function. *Journal of statistical planning and inference* 90, 2 (2000), 227–244.

[31] Baochen Sun and Kate Saenko. 2016. Deep coral: Correlation alignment for deep domain adaptation. In *Computer Vision–ECCV 2016 Workshops: Amsterdam, The Netherlands, October 8-10 and 15-16, 2016, Proceedings, Part III 14*. Springer, 443–450.

[32] Vladimir Vapnik. 1999. *The nature of statistical learning theory*. Springer science & business media.

[33] Jindong Wang, Cuiling Lan, Chang Liu, Yidong Ouyang, Tao Qin, Wang Lu, Yiqiang Chen, Wenjun Zeng, and Philip Yu. 2022. Generalizing to unseen domains: A survey on domain generalization. *IEEE Transactions on Knowledge and Data Engineering* (2022).

[34] Ke Wang, Senqiang Zhou, Chee Ada Fu, and Jeffrey Xu Yu. 2003. Mining changes of classification by correspondence tracing. In *Proceedings of the 2003 SIAM International Conference on Data Mining*. SIAM, 95–106.

[35] Wenhao Wang, Shengcai Liao, Fang Zhao, Cuicui Kang, and Ling Shao. 2020. Domainmix: Learning generalizable person re-identification without human annotations. *arXiv preprint arXiv:2011.11953* (2020).

[36] Gerhard Widmer and Miroslav Kubat. 1996. Learning in the presence of concept drift and hidden contexts. *Machine learning* 23 (1996), 69–101.

[37] Shen Yan, Huan Song, Nanxiang Li, Lincan Zou, and Liu Ren. 2020. Improve unsupervised domain adaptation with mixup training. *arXiv preprint arXiv:2001.00677* (2020).

[38] Rich Zemel, Yu Wu, Kevin Swersky, Toni Pitassi, and Cynthia Dwork. 2013. Learning fair representations. In *International conference on machine learning*. PMLR, 325–333.

[39] Hanlin Zhang, Yi-Fan Zhang, Weiyang Liu, Adrian Weller, Bernhard Schölkopf, and Eric P Xing. 2022. Towards principled disentanglement for domain generalization. In *Proceedings of the IEEE/CVF Conference on Computer Vision and Pattern Recognition*. 8024–8034.

[40] Chen Zhao. 2021. *Fairness-Aware Multi-Task and Meta Learning*. Ph. D. Dissertation.

[41] Chen Zhao, Feng Chen, and Bhavani Thuraisingham. 2021. Fairness-aware online meta-learning. In *Proceedings of the 27th ACM SIGKDD Conference on Knowledge Discovery & Data Mining*. 2294–2304.

[42] Chen Zhao, Feng Mi, Xintao Wu, Kai Jiang, Latifur Khan, and Feng Chen. 2022. Adaptive fairness-aware online meta-learning for changing environments. In *Proceedings of the 28th ACM SIGKDD Conference on Knowledge Discovery and Data Mining*. 2565–2575.

[43] Chen Zhao, Feng Mi, Xintao Wu, Kai Jiang, Latifur Khan, and Feng Chen. 2024. Dynamic Environment Responsive Online Meta-Learning with Fairness Awareness. *ACM Transactions on Knowledge Discovery from Data* 18, 6 (2024), 1–23.

[44] Chen Zhao, Feng Mi, Xintao Wu, Kai Jiang, Latifur Khan, Christan Grant, and Feng Chen. 2023. Towards Fair Disentangled Online Learning for Changing Environments. In *Proceedings of the 29th ACM SIGKDD Conference on Knowledge Discovery and Data Mining*. 3480–3491.